Rev. Adv. Mater. Technol., 2023, vol. 5, no. 2, pp. 10–24 DOI: 10.17586/2687-0568-2023-5-2-10-24

Preparation of Ga_2O_3 Thin Films by Sol-Gel Method—a Concise Review

X. Zhang[1,*], V.A. Spiridonov[1], D.I. Panov[1], I.M. Sosnin[1,2], A.E. Romanov[1,2,3]

[1] ITMO University, Kronverkskiy pr., 49, lit. A, Saint Petersburg, 197101, Russia
[2] Togliatti State University, Belorusskaya, 14, Togliatti, 445020, Russia
[3] Ioffe Institute, Polytechnicheskaya str., 26, Saint Petersburg 194021, Russia

Article history

Received May 29, 2023
Accepted June 10, 2023
Available online June 30, 2023

Abstract

Nowadays, gallium oxide (Ga_2O_3) as a wide bandgap semiconductor material is acquiring more and more attention in various practical areas. As a result, there has been a lot of efforts to fabricate and study bulk Ga_2O_3 material, Ga_2O_3 thin films, and Ga_2O_3 nanowires. For Ga_2O_3 films, there exists a variety of preparation methods such as metal-organic chemical vapor deposition, hydride vapor phase epitaxy, pulsed laser deposition, molecular beam epitaxy, frequency magnetron sputtering, atomic layer deposition, wet chemistry, and sol-gel. This concise review focuses on the preparation of Ga_2O_3 thin films by sol-gel methods. Sol-gel methods include dip-coating, spin-coating, spray pyrolysis, and drop casting technique. The details on the fabrication of β-Ga_2O_3 thin films by sol-gel method are summarized and prospected. Polymorphism, structure and properties of sol-gel prepared Ga_2O_3 films are discussed.

Keywords: Sol-gel; Ga_2O_3; Thin film

CONTENTS

1. Introduction 10
2. Basic properties of Ga_2O_3 11
   2.1. Polymorphism of Ga_2O_3 11
   2.2. Crystal Structure of β-Ga_2O_3 11
   2.3. Properties of β-Ga_2O_3 12
3. Ga_2O_3 film preparation 14
   3.1. Sol-Gel method history 14
   3.2. Sol-gel method principle 14
   3.3. Common coating techniques 15
      3.3.1. Dip-coating 15
      3.3.2. Spin-coating 16
      3.3.3. Spray-pyrolysis 17
      3.3.4. Drop casting 17
   3.4. Different polymorphs of Ga_2O_3 obtained by sol-gel method 19
4. Applications in brief 19
5. Conclusion 20
References 20

1. INTRODUCTION

Wide bandgap ($E_g > 2.2$ eV) semiconductor materials such as SiC (3.25 eV), GaN (3.4 eV), ZnO (3.37 eV) are widely used in lighting, optical storage, high-frequency and high-power electronic devices due to their superior optical and electrical properties [1–4]. Ultra-wide bandgap ($E_g > 4$ eV) semiconductor materials such as Ga_2O_3 (4.2–5.0 eV), diamond (5.5 eV), and AlN (6.2 eV) with larger bandgap widths have superior physical properties, such as high breakdown electric field strength, excellent dielectric constant, stable high-temperature performance, and low energy loss [5–7].

Ga_2O_3 belongs to the transparent semiconducting oxides (TSOs) and has a long research history. In 1875 Lecoq de Boisbaudran discovered the element gallium and its compounds [8]. In 1952 Roy et al. first reported the phase equilibrium of the Al_2O_3-Ga_2O_3-H_2O system and identified the different forms of Ga_2O_3 and their stability [9]. The early research was mainly about the basic

* Corresponding author: X. Zhang, e-mail: 314519083@qq.com

© ITMO University, 2023

properties of Ga_2O_3, and the later research explored practical use of this material in power devices, but also from the perspectives of optoelectronics and sensorics. Ga_2O_3 has remarkable properties in electrical, optical, chemical, and other aspects and is suitable for mass production of electronic and optoelectronic devices. Its band gap and Baliga's figure of merit (FOM) are much larger than those of GaN and SiC; Ga_2O_3 demonstrates high breakdown voltage (V_{br}); it has unique advantages in optoelectronic devices, solar-blind ultraviolet photodetectors, and high-power, low-loss devices [10–14].

Ga_2O_3 can be obtained as a bulk crystal. The most common techniques utilize the growth from melt by Czochralski (CZ) method [15] and Edge defined film-fed growth (EFG) or Stepanov' technique [16]. Ga_2O_3 crystalline films can be fabricated with various techniques, such as metal-organic chemical vapor deposition (MOCVD) [17], hydride vapor phase epitaxy (HVPE) and pulsed laser deposition (PLD) [18], molecular beam epitaxy (MBE) [19,20], radio frequency magnetron sputtering (RFMS) [21,22], atomic layer deposition (ALD) [23,24], and sol-gel method [25–27]. The sol-gel method is less expensive, more convenient, and easier to control composition and uniformity than other methods. In this article, we focus on the preparation of Ga_2O_3 thin films by sol-gel method and briefly discuss the properties of sol-gel fabricated Ga_2O_3films.

2. BASIC PROPERTIES OF GA_2O_3

2.1. Polymorphism of Ga_2O_3

Ga_2O_3 is currently confirmed to have six different polymorphs, α, β, γ, δ, ε, κ, as shown in Table 1 [9,14,28–30]. The crystal structure and coordination number of Ga ions in different phases of Ga_2O_3 are different, and its lattice parameters, crystal structure and properties will also change accordingly. Formation of a particular phase greatly depends on the substrate (in the case of films) and growth temperature. Among listed polyforms, κ- phase is a transient one and β- phase is the most stable [30], δ-phase is a mixture of β- and ε-phases [31], ε-phase may be more like κ-phase due to the formation of misoriented grains on a sapphire substrate [32].

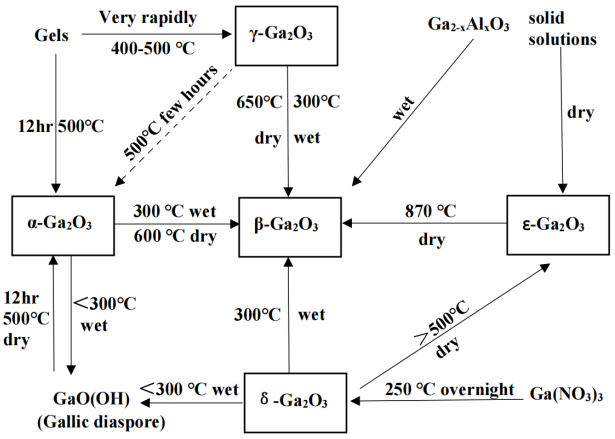

Fig. 1. Conversion relationship between Ga_2O_3 polymorphs. Reprinted with permission from Ref. [9], © 2022 American Chemical Society.

α-Ga_2O_3 is in a hexagonal crystal system and has the corundum crystal structure. It can be prepared on sapphire substrates at rather low deposition temperatures and demonstrates band gap values up to ~5.1 eV [36–38]. The α-phase is widely used in power devices and optoelectronic applications due to its largest band gap [39], and the ε-phase and γ-phase have also been reported as solar-blind UV detectors. There are also sporadic reports on δ-phase and κ-phase, but the research focus is not in the field of optoelectronics [40]. Most of the literature reports are about β-Ga_2O_3 properties and applications. Various crystal forms of Ga_2O_3 will transform into β-Ga_2O_3 at high temperatures, and the transformation route has been clearly described as early as in 1952 [9]. In addition to β-Ga_2O_3, α-phase and ε-Ga_2O_3 are relatively stable, while γ- and δ-Ga_2O_3 can easily transform into other crystal forms. Figure 1 shows the conversion relationship between Ga_2O_3 polymorphs. The research works discussed in this paper are mainly based on β-Ga_2O_3, so in the next two subsections, the properties of β-Ga_2O_3 are considered in more details.

2.2. Crystal Structure of β-Ga_2O_3

β-Ga_2O_3 belongs to the monoclinic crystal system (C2/m), and the unit cell is composed of two kinds of gallium ions

Table 1. Ga_2O_3 polymorphs.

Polymorph	Structure	Space group	Lattice parameters	Ref.
α	Rhombohedral	$R\bar{3}c$	$a = b = 4.98$ Å, $c = 13.43$ Å, α = β = 90°, γ = 120°	[33]
β	Monoclinic	$C2/m$	$a = 12.23$ Å, $b = 3.04$ Å, $c = 5.80$ Å, α = γ = 90°, β = 103.8°	[34]
γ	Cubic (spinel)	$Fd\bar{3}m$	$a = b = c = 8.24$ Å, α = β = γ = 90°	[31]
δ	Cubic (bixbyite)	$Ia3$	$a = b = c = 9.52$ Å, α = β = γ =90°	[35]
ε	Hexagonal	$P63mc$	$a = b = 2.90$ Å, $c = 9.26$ Å, α = β = 90°, γ=120°	[30]
κ	Orthorhombic (transient)	$Pna2_1$	$a = 5.05$ Å, $b = 8.70$ Å, $c = 9.28$ Å,α = β = γ =90°	[32]

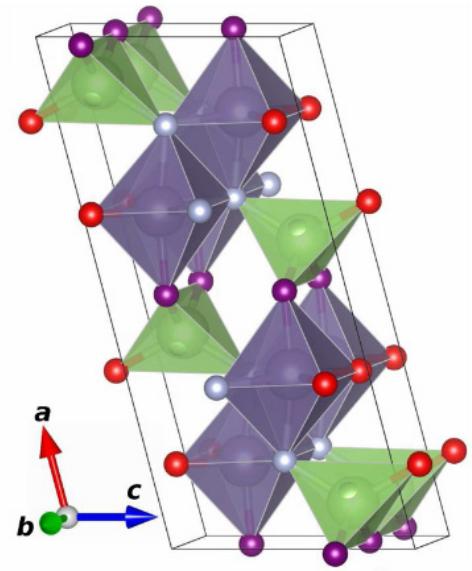

Fig. 2. Crystal structure of β-Ga_2O_3. Reprinted with permission from Ref. [41], © 2015 WILEY-VCH Verlag GmbH & Co. KGaA, Weinheim.

and three kinds of oxygen atoms. Figure 2 shows the crystal structure of β-Ga_2O_3 [41]. The lattice constants *a*, *b*, *c*, and angle β are 12.23 Å, 3.04 Å, 5.80 Å, and 103.7°, respectively. The unit cell is composed of four Ga_2O_3 building blocks. Each unit cell contains two different Ga ions (Ga_I and Ga_{II}), and three O ions (O_I, O_{II}, and O_{III}). The crystal structure can be described by the connections between GaO_6 octahedra and GaO_4 tetrahedra. Due to this crystal lattice configuration, strong physical anisotropy is observed experimentally and predicted theoretically. The thermal conductivity of β-Ga_2O_3 along the [010] direction is twice as large as that in the [100] direction [42,43], while studies have shown that the difference in electron effective mass (m_e) between these two directions is not significant [41,44,45]. Due to the connection relationship between GaO_6 octahedron and GaO_4 tetrahedron in the unit cell, the carrier mobility along the *b*-axis direction is higher than in other crystallographic directions.

2.3. Properties of β-Ga_2O_3

Due to its wide band gap, β-Ga_2O_3 is highly transparent in the visible and ultraviolet parts of the electromagnetic spectrum, and the intrinsically pure β-Ga_2O_3 is colorless and transparent. However, due to impurities and defects that may be introduced during the crystal growth process, β-Ga_2O_3 crystals may exhibit specific colors. Galazka et al. [46,47] found a strong correlation between the electrical conductivity and optical properties of β-Ga_2O_3: insulating β-Ga_2O_3 crystals are colorless or light blue. Due to the increase of electron concentration, the *n*-type conductive crystal absorbs red light; near-infrared bands also

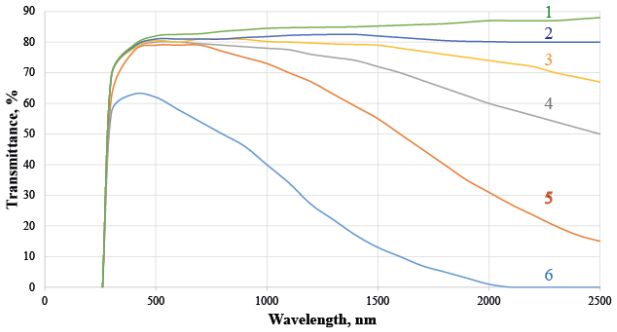

Fig. 3. Optical transmission spectra of β-Ga_2O_3 single crystals with different electron concentrations: 1 – insulating (doped with Mg); 2 – 4×10^{16} cm^{-3}; 3 – 3.5×10^{17} cm^{-3}; 4 – 5.2×10^{17} cm^{-3}; 5 – 2.2×10^{18} cm^{-3}; 6 – 1×10^{19} cm^{-3} (Sn). Reprinted from Ref. [14].

contribute stronger, so crystals become slightly blue, while the light gray color of β-Ga_2O_3 crystals is caused by unintentional doping with C atoms. Figure 3 shows the optical transmission spectra of β-Ga_2O_3 single crystals with different electron concentrations, in which the samples with low electron concentrations show a steep intrinsic absorption at 255–260 nm, and when the wavelength is greater than 260 nm, the samples show a high optical transmittance (≥80%). As the electron concentration increases, the transmittance of β-Ga_2O_3 in the visible and near-infrared regions decreases significantly.

The absorption spectrum of β-Ga_2O_3 typically has rather sharp absorption cut-off edge at 255–260 nm and two absorption shoulders at around 270 nm and 300 nm [46]. The absorption cutoff edge at 255–260 nm is attributed to the intrinsic transition of electrons from the valence band to the conduction band [48]. Ueda et al. [49] found that the absorption of photons by β-Ga_2O_3 is related to the polarization direction of the incident light. When the polarization direction is parallel to the *b* and *c*-axes, the corresponding intrinsic absorption limits are 253 and 270 nm respectively [49]. In the energy band structure, they correspond to transitions from the high symmetry point Γ_{2^-} of the valence band to Γ_{1^-} of the conduction band, and transitions from Γ_{1^-} of the valence band to Γ_{1^+} of the conduction band. However, this model cannot explain the experimentally observed discrepancy between the absorption and excitation spectra. Villora et al. [50] believe that the absorption at 270 nm is due to the transition of electrons from the valence band to the conduction band disturbed by Ga^{3+} vacancies, while the absorption at 260 nm is caused by the transition of electrons from the valence band to the conduction band.

β-Ga_2O_3 has three different luminescence bands, which are ultraviolet (3.2–3.6 eV), blue (2.8–3.0 eV), and green (2.4 eV) luminescence bands [51,52]. The luminescence is due to the radiative annihilation of carriers at self-trapped excitons or carrier annihilation assisted by lattice

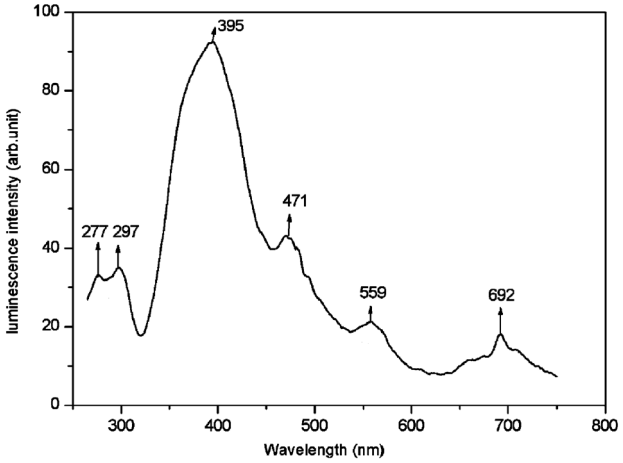

Fig. 4. Luminescence spectra of β-Ga_2O_3 single crystal excited by xenon light at 254 nm. Adapted from Ref. [48].

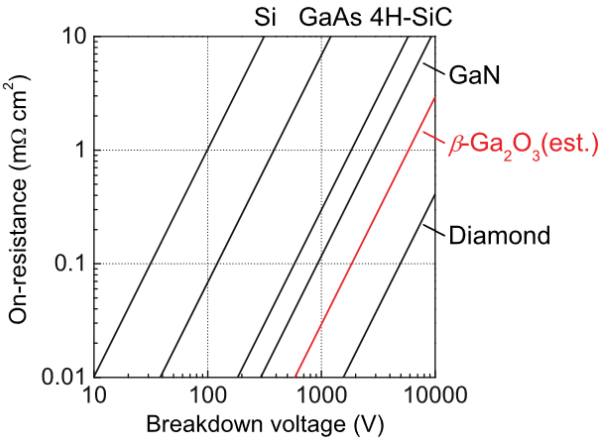

Fig. 5. Comparison of breakdown field and on-resistance of high-power device materials. Reprinted with permission from Ref. [57], © 2012 AIP Publishing LLC.

defects [53]. The UV luminescence band is not related to the preparation method of β-Ga_2O_3 and the type of impurities. As shown in Figure 4, it is visible in the luminescence spectrum of β-Ga_2O_3 single crystal excited by 254 nm xenon light source [48]. Considering the value of the band gap of β-Ga_2O_3, the generation of the UV luminescence band does not originate from a direct jump between the conduction band and the valence band, but probably from a complex between the free electrons and the bound polarized holes in the material [52]. The blue luminescence intensity is related to the resistivity of the sample material, implying that it is most likely related to the oxygen vacancies that lead to the *n*-type conducting characteristics of the sample [54]. Harwig and Kellendonk [51] supposed that the blue light originates from the recombination of electrons provided by donor impurities (possibly oxygen vacancies or gallium interstitial atoms) and holes provided by acceptor impurities (gallium vacancies or gallium-oxygen vacancy pairs) in the material. The green luminescence band is related to the specific doping elements in β-Ga_2O_3; e.g., Villora et al. believed that the green luminescence is related to the bound excitons [50].

Table 2 shows the comparison of basic characteristic parameters between β-Ga_2O_3 and current mainstream semiconductor materials [55,56]. The Baliga's FOM is used to comprehensively evaluate the application value index of semiconductor materials in power devices. In addition to being related to the breakdown electric field strength, it is also affected by electron mobility and dielectric constant. The Baliga's FOM of β-Ga_2O_3 reaches 3444 due to its larger band gap, which is much larger than that of SiC (340) and GaN (870), which are representative materials of the third-generation semiconductors.When β-Ga_2O_3 is used in power devices, the maximum breakdown electric field strength E_{br} can reach 8 MV/cm. The Baliga's FOM is a basic parameter that indicates that the material is suitable for power devices, which is proportional to the cube of E_{br} and linearly proportional to electron mobility μ. Therefore, high E_{br} is an excellent characteristic of Ga_2O_3. According to the function relationship between the on-resistance and the maximum breakdown voltage, the conduction loss of β-Ga_2O_3 is much lower than that of SiC and GaN under the same electric field strength as Figure 5 [57] shows. When the carrier (electron) concentration is 10^{15}–10^{16} cm^{-3}, the electron mobility μ of β-Ga_2O_3 measured in the experiment is 300 $cm^2 \cdot V^{-1}s^{-1}$ [58]. Compared with the high-temperature (greater than 2000 °C) sublimation method used in the preparation of SiC substrates, and the high-pressure

Table 2. Comparison of parameters between β-Ga_2O_3 and main semiconductor materials.

Material	Bandgap, E_g (eV)	Electron mobility, μ ($cm^2 \cdot V^{-1}s^{-1}$)	Breakdown field, E_{br} (MV/cm)	Relative dielectric constant, ε	Baliga's FOM	Thermal conductivity, λ ($W \cdot m^{-1} \cdot K^{-1}$)
Si	1.1	1400	0.3	11.8	1	150
GaAs	1.4	8000	0.4	12.9	15	55
4H-SiC	3.3	1000	2.5	9.7	340	270
GaN	3.4	1200	3.3	9.0	870	210
Diamond	5.5	2000	10	5.5	24664	1000
β-Ga_2O_3	4.9	300	8	10	3444	13 along [100] (Ref. [43]) 21 along [010] (Ref. [42])

nitrogen method, ammonothermal technology method, and hydride vapor phase epitaxy method used in the preparation of GaN substrates, β-Ga_2O_3 single crystals can be directly produced with inexpensive and stable methods for mass growth [57]. Therefore, β-Ga_2O_3 is very likely to become a star material for the next generation of power semiconductor devices.

β-Ga_2O_3 is a poor conductor of heat compared to other semiconductors as Table 2 shows. The following equation was used to fit temperature dependent thermal conductivity κ data in two temperature ranges (80–200 K and 200–495 K):

$$\kappa(T) = AT^{-m}. \tag{1}$$

The exponent *m* is about 3.5 in the low temperature range (80–200K) and about 1.2 in the high temperature range (200–495K) [61]. At low temperatures, there is a large gap between the actual conductivity and the typical $T^{-3/2}$ dependence, suggesting that heat conduction is limited by free electron and phonon scattering [42,59].

As was already mentioned β-Ga_2O_3 belongs to the monoclinic crystal system. This means that β-Ga_2O_3 has thirteen independent elastic stiffness constants C_{ij}:

$$\left[C_{ij}\right] = \begin{bmatrix} C_{11} & C_{12} & C_{13} & 0 & C_{15} & 0 \\ & C_{22} & C_{23} & 0 & C_{25} & 0 \\ & & C_{33} & 0 & C_{35} & 0 \\ & & & C_{44} & 0 & C_{46} \\ & sym. & & & C_{55} & 0 \\ & & & & & C_{66} \end{bmatrix}. \tag{2}$$

As a result, β-Ga_2O_3 has strong longitudinal modulus anisotropy ($C_{11} \ll C_{22}$, C_{33}) and strong shear modulus anisotropy. These anomalous elastic properties are only present in the specific space group C2/m, while monoclinic materials with other space groups do not possess these properties [60]. The strong longitudinal modulus anisotropy indicates that β-Ga_2O_3 has a weaker chemical bond in the [100] direction, which implies that β-Ga_2O_3 is more compressible along the *x*-axis than along the *y*- and *z*-axes [61]. In general, most of the elastic stiffness constants of β-Ga_2O_3 increase as the pressure becomes larger when the hydrostatic pressure is less than 15 GPa. However, at pressures between 15 and 20 GPa, most of the elastic stiffness constants behave abnormally, indicating that the monoclinic phase starts to transform into the rhombohedral phase (α-Ga_2O_3) [61].

3. Ga_2O_3 FILM PREPARATION

3.1. Sol-gel method history

Kistler reported the preparation of aerogels back in 1931 [62], and although the term "sol-gel" did not exist at the time, these aerogels are considered the first sol-gel products. In 1969 high-purity barium titanate powder was prepared from barium and titanium alkoxides by Mazdiyasni et al. [63]. And in the same year Roy made small silica glass flakes by heating gelatinized water glass [63]. The International Sol-Gel Symposium, held regularly since 1981, and the Journal of Sol-Gel Technology, founded in 1993, are the main sources of scientific information in the field. Initial research focused on silica and silicate glasses, but later extended to other oxide and non-oxide ceramics and composites. The studies conducted have shown that sol-gel methods can produce the materials at relatively low temperatures in the form of sheets, fibers, bulk samples, and coating films or layers. With sol-gel method, it is also possible to advance new composition materials with high purity and homogeneity. Sol-gel method allows to control the particle size and size distribution to the nanoscale level [64]. In 1998 Yada et al. [65] used the sol-gel method for the preparation of Ga_2O_3 for the first time.

3.2. Sol-gel method principle

The sol-gel method is a chemical method. When preparing a coating, a metal alkoxide or an inorganic salt is used as a precursor, which is dissolved in a solvent (water or organic solvent) to form a uniform solution. The solute and the solvent will undergo hydrolysis or alcoholysis reaction, and the reaction product will be aggregated into particles with a size of several nanometers to form a sol. The sol is then coated on various substrates in a certain way, and the sol film is gelled and dried to obtain a xerogel film. Finally, according to the different raw materials and requirements, annealing is performed at the appropriate temperature to obtain the desired coating [66]. The steps for preparation process of the sol-gel method are shown schematically in Figure 6.

According to different precursor raw materials, the method utilizes either inorganic salt hydrolysis or alcohol salt hydrolysis. At present, the method of alkoxide hydrolysis is mostly used. After dissolving the metal alkoxide in an organic solvent, a hydrolysis reaction and a polycondensation reaction occur to form the required sol. The prepared sol is smeared and then dried and sintered at a certain temperature to form a film with certain properties. During the heating process, the gel first removes the water and alcohol on the surface at a lower temperature, and then the OR (where R denotes the alkyl hydroxyl group.) group is oxidized at a moderate temperature, and the OH group is removed above 300 °C to form a film. The whole process can be expressed as following reactions [67].

1) Hydrolysis reaction. Metal alkoxides react chemically with water to produce hydroxyl groups:

$$\mathrm{M(OR)}_n + x\mathrm{H_2O} \rightarrow \mathrm{M(OH)}_x\mathrm{(OR)}_{n-x} + x\mathrm{ROH}. \tag{3}$$

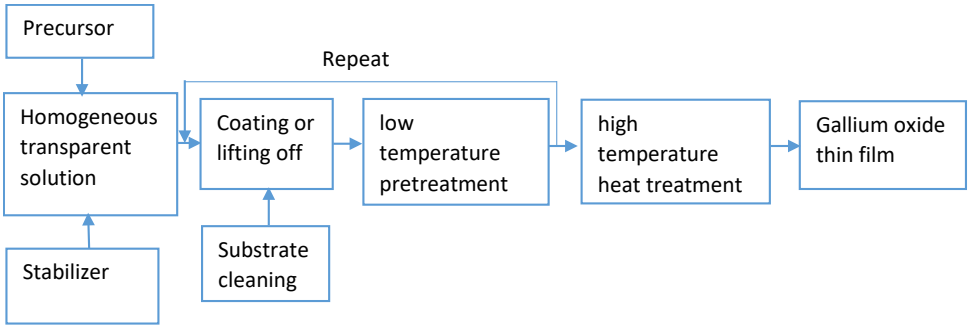

Figure 6. Schematic diagram of the process principle of Ga_2O_3 film prepared by sol-gel method.

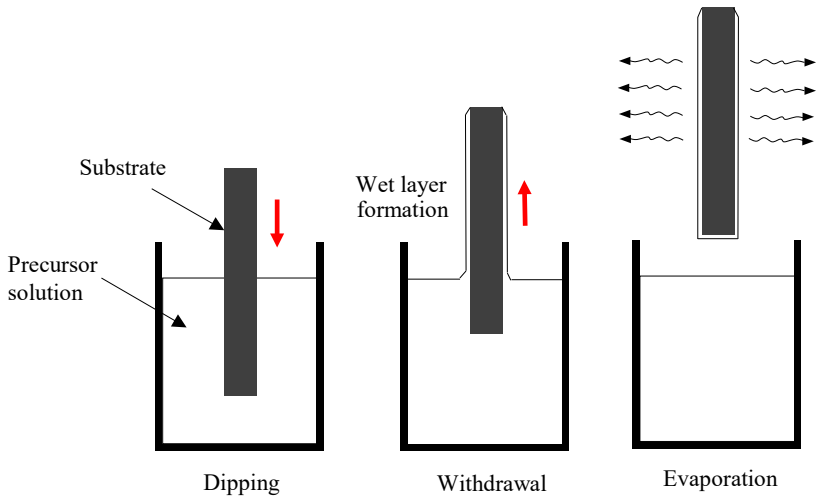

Figure 7. Schematic diagram of the principle of dip coating. Adapted from Ref. [69].

2) Polycondensation reaction. The hydroxyl group produced in the first step undergoes water loss, see Eq. (4), or alcohol loss, see Eq. (5):

$$-M-OH+HO-M- \rightarrow -M-O-M-+H_2O, \quad (4)$$

$$-M-OR+HO-M- \rightarrow -M-O-M-+ROH. \quad (5)$$

3) Heating process. After the reactions of the first two steps, keeping it at a certain temperature will prompt it to continue to react to form a polymer. Further hydrolysis reactions will follow and will increase the degree of polymerization, eventually forming a gel:

$$-M-OR+M-OR \rightarrow -M-O-M-+ROR. \quad (6)$$

During the whole solution preparation process, the sol concentration, aging time, and heat treatment temperature all have certain influences on the quality of the final film. In the process of film preparation, there will also be reactions caused by solvent evaporation, which will change the properties of the film. During the heat treatment of film drying, the rapid evaporation of water and organic solvents in the sol will cause volume shrinkage and can easily lead to cracking of the film. Therefore, during the experiment, it is necessary to pay close attention to these influencing factors to ensure the quality of the prepared film [68].

3.3. Common coating techniques

Annealing is one of the most important processes in sol-gel manufacturing because heating and cooling removes defects in materials to improve their structural properties. β-Ga_2O_3 is an ultra-wide bandgap material with semiconducting properties. Oxygen defects can be removed by high temperature annealing process. Compared with other methods, the sol-gel method does not require vacuum conditions, and this method provides low costs in large-scale applications. Compared with other existing fabrication methods, the gallium oxide films prepared by the sol-gel method have advantages in economy and other aspects [27].

3.3.1. Dip-coating

Figure 7 shows a schematic diagram of the dip-coating method. The substrate is dipped directly into the sol and then the solution is lowered (or the substrate is lifted) so that the sol adheres to the substrate. After drying the sample in a specific temperature environment, a thin film is formed. During the experiments, the sol concentration, sol viscosity, immersion time, pulling or moving speed all affect the quality of the film, which needs to be

continuously explored and improved. However, throughout the pulling process of this coating method, droplets will be formed downward due to the surface tension of the liquid, and then a certain thickness step will be observed. In this technique, both sides of the substrate are coated with sol, which also affects the transmittance of the obtained samples.

Minami et al. [70] demonstrated Ga_2O_3:Mn thin films made by dip coating and developed high-luminance electroluminescent devices. They dissolved $Ga(C_5H_7O_2)_3$ and $MnCl_2$ in CH_3OH and stirred in N_2 gas atmosphere; 30 minutes later, H_2O and HCl were added to the solution, and the desired solution was prepared by stirring under N_2 gas and 50 °C atmosphere for 5 hours. Then the $BaTiO_3$ ceramic sheets were immersed in the solution, taken out and dried in the air for about 5 minutes. After that the sample was placed in 600–1000 °C atmosphere for 10 minutes to obtain a thin film. The procedure was repeated 25 times, and finally the film of about 2μm thickness was obtained. The Ga_2O_3:Mn film was annealed in an Ar atmosphere at 850–1070 °C for 1 hour and demonstrated an amorphous nature. They found that the Thin-film electroluminescent (TFEL) devices made with this method exhibited luminances of 1271 and 401 cd/m^2 when driven by 1 kHz and 60 Hz sinusoidal electric waves, respectively. Therefore, the production of lower-cost oxide phosphor TFEL displays and flat-panel TFEL lamps by sol-gel dip-coating route has broad prospects.

Mohammadi et al. [71] used dip-coating method to synthesize mesoporous TiO_2-Ga_2O_3 films on quartz and alumina substrate with different Ti:Ga atomic ratios. In the experiments, gallium (III) nitrate hydrate and titanium isopropoxide were used as precursors, and hydroxypropyl cellulose (HPC) was used as a polymeric fugitive agent (PFA) to increase the specific surface area (SSA). It was found that introducing Ga_2O_3 into the TiO_2 film can reduce the average grain size of the material. After annealing at 600 °C, TG11 (Ti:Ga = 1:1) has the smallest grain size of all films, which is 19 nm. They also found that the TG11 sample has the smallest grain size and the largest roughness after annealing at 600 °C. After annealing at 800 °C, the average grain size of all samples is about 32 nm with the decreased sample roughness.

Sinha et al. [72] dissolved gallium metal in hydrochloric acid, and then dehydrated the solution to obtain a white precipitate, which was added to absolute ethanol at a ratio of 0.075 mole L^{-1}. The solution was continuously stirred and a few drops of acetic acid were added until the solution became clear. They used the dip-coating method to cover the sol on the cleaned amorphous quartz substrate, and finally annealed the film at 700 °C for 1 hour to obtain a uniform Ga_2O_3 film [72].

3.3.2. Spin-coating

Spin coating method is to fix the substrate on the homogenizer, and then put the prepared sol on the substrate. The centrifugal force generated by the high-speed rotation of the homogenizer table spreads the sol from the center outward and evenly coats the substrate, which can form a thin film initially, as shown in Figure 8. Then, the vacuum pump is turned off, and the substrate can be removed for heat treatment to form the desired film. The concentration of sol and the choice of substrate material will affect the quality and thickness of the film. Parameters such as the rotation speed, time, and drop volume of the homogenizer also need to be tested repeatedly to prepare high-quality films.

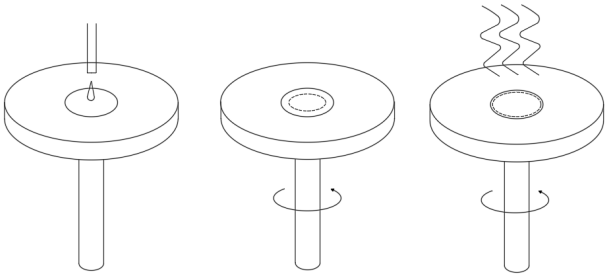

Fig. 8. Schematic diagram of spin coating technique.

Zhu et al. [26] successfully synthesized β-Ga_2O_3 thin film on (0001) sapphire substrate by spin coating technique. They dissolved $Ga(NO_3)_3{\cdot}xH_2O$ in ethanol, stirred at room temperature and added monoethanolamine (MEA; C_2H_7NO) to obtain the desired solution with molar concentration of 0.4 mol/L, and the molar ratio of MEA and $Ga(NO_3)_3{\cdot}xH_2O$ was 1.0. Then they spin-coated the solution on the cleaned (0001) sapphire substrate, and preheated the sample in an O_2 atmosphere at 100–500 °C for 10 minutes. This step was repeated five times to reach the desired thickness of the film. Finally, the sample was post-annealed at 1000 °C to form the β-Ga_2O_3 film. They found that when the preheating temperature was 100 °C and 200 °C, there were cracks on the surface of the synthesized β-Ga_2O_3 film. However, when the preheating temperature was 300–500 °C, the fabricated film had no cracks and was very flat. When the preheating temperature was increased from 100 °C to 400 °C, the surface of the film became smoother and denser, which was due to the effect of the treatment temperature on the surface free energy [73].

Kokubun et al [74] synthesized β-Ga_2O_3 films on sapphire substrate by spin coating technique. They investigated the effect of annealing temperature on the spectral response of the photodetector. As shown in Figure 9, when the annealing temperature was 600 and 800 °C, the photocurrent peak appeared for 250 nm radiation

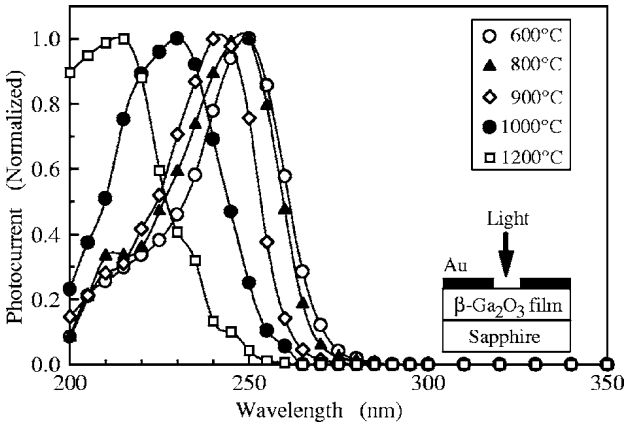

Fig. 9. Spectral response of β-Ga_2O_3 photodetectors fabricated at different annealing temperatures. Reproduced with permission from Ref. [74], © 2007 AIP Publishing.

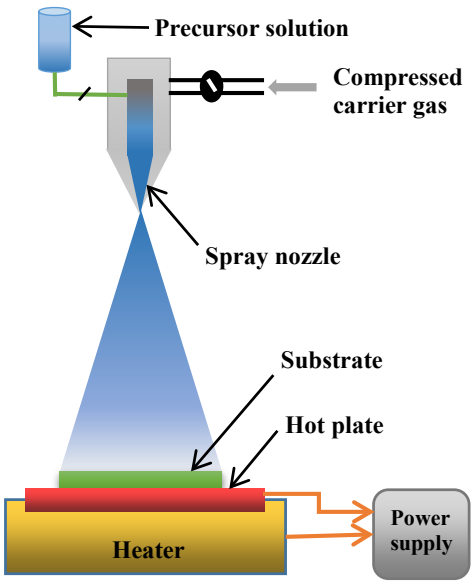

Fig. 10. Schematic diagram of the experimental device for spray pyrolysis. Adapted from Ref. [79].

wavelength, and no photocurrent for wavelengths larger than 280 nm was observed. When the annealing temperature exceeds 900 °C, the photocurrent peak shifts to shorter wavelengths. The maximum value of the responsivity ~8×10^{-5} A/W occurred during the annealing of the film at 1000 °C. It was argued that when the annealing temperature increases above 900 °C, the lattice constant of the film material decreases and the band gap increases. The authors believe this is due to the diffusion of aluminum from the sapphire substrate to the Ga sites in the β-Ga_2O_3 lattice [74]. This phenomenon has also been described elsewhere in the literature [75–77].

It is useful to note that the sol-gel method is easy to use for the doping of Ga_2O_3 thin films. Y. Li et al. [78] prepared Ga_2O_3 films doped with Ce, Sb, W and Zn by spin coating. Then these dopped layers were used to make gas sensors with semiconductor thin films.

3.3.3. Spray-pyrolysis

Compared with the first two techniques mentioned above, the spraying method is more suitable for large-scale industrial production of Ga_2O_3 films. Spray pyrolysis equipment consists of a precursor solution tank, an atomizer, a substrate heater and a temperature controller [79]. A typical experimental setup for spray pyrolysis is shown schematically in Figure 10.

Atomizers are usually available in different spray pyrolysis techniques: blast (liquid exposed to a stream of air) [79,80], ultrasonic spray pyrolysis [81] and electrostatic spray deposition (EDS) [82].

The properties of produced by this technique films are affected by many factors such as the ratio of anions to cations, the spraying rate, the temperature of the substrate, the ambient atmosphere, the carrier gas, the droplet size, and the cooling rate. The distance between the nozzle and the substrate, the temperature of the substrate, the concentration of the precursor solution, and the amount of precursor solution sprayed all affect the film thickness [79]. Film thickness is also controlled by sol concentration, flow rate, viscosity, pressure, spray gun speed and spraying time [83]. The coating process seems simple, but it has high requirements for equipment, high cost, and relatively low reusability of spray liquid, so it is only suitable for industrial spraying of specific materials.

We have prepared Ga_2O_3 thin films on silica glass (SiO_2) substrates by spray-pyrolysis method which was described in our article [84]. To obtain the sol we dissolved gallium nitrate [$Ga(NO_3)_3{\cdot}8H_2O$] (99.9%) in ethylene glycol [$C_2H_6O_2$] (99.5%), added monoethanolamine [C_2H_7NO] (99.5%) as a stabilizer. The sol heated by the high-temperature furnace was sprayed directly onto the substrate preheated to the same high temperature. Used spraying equipment was suitable to form a film at flat surfaces. The operation process is schematically presented in Figure 11. As Figure 12 shows, the prepared β-Ga_2O_3 thin films had some cracks, which may be caused by the difference in thermal expansion coefficient between the thin film and the substrate. After the sample was annealed at 900 °C, the transmittance of the film increased, and the estimated band gap of the semiconductor material was determined as 4.87 eV (Fig. 13).

3.3.4. Drop casting

As shown in Figure 14, drop casting is a simple film-forming technique in which a prepared mixture is cast directly on a substrate and then the solvent is evaporated. This technique is similar to spin coating, but does not require substrate rotation. In this technique it is difficult to

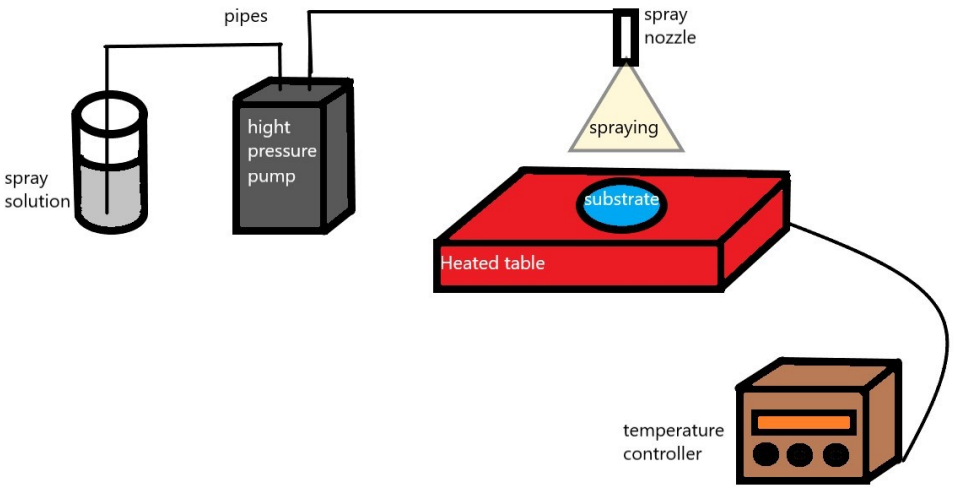

Fig. 11. Schematic diagram of spray-pyrolysis technique. Adapted from Ref. [84].

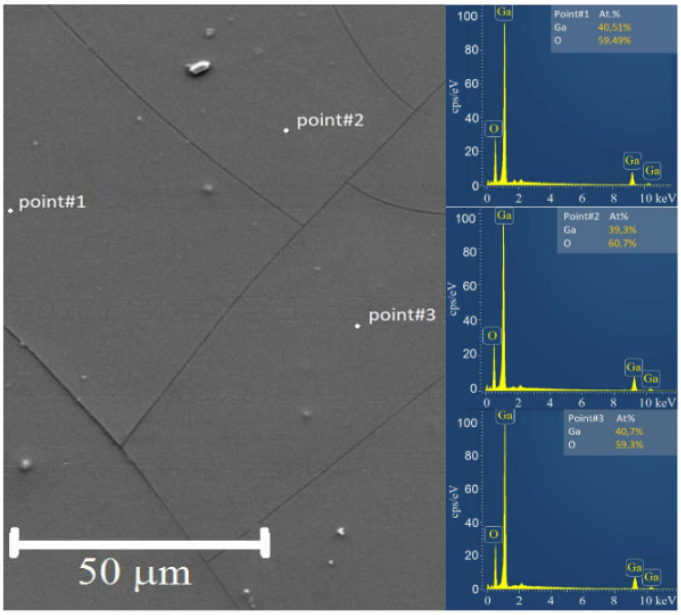

Fig. 12. SEM image and EDX measured composition of the sol-gel prepared β-Ga_2O_3 film. Adapted from Ref. [84].

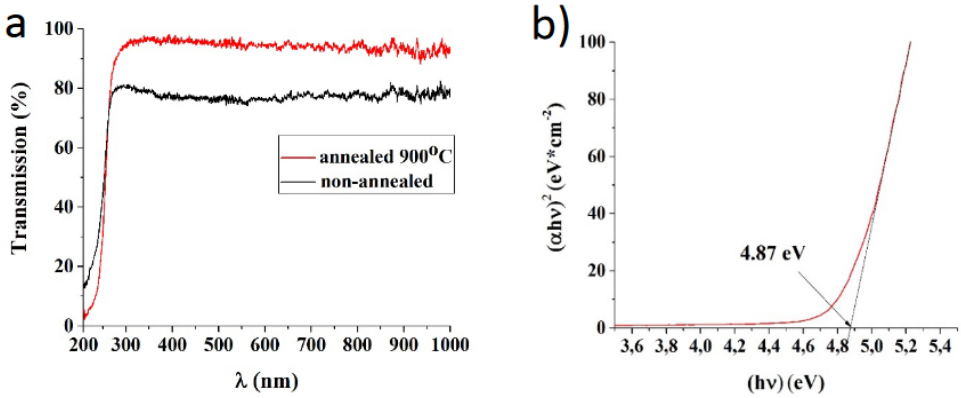

Fig. 13. Properties of sol-gel fabricated β-Ga_2O_3 films; (a) transmittance of the film (b) estimated bandgap of the film material after annealing at 900 °C. Adapted from Ref. [84].

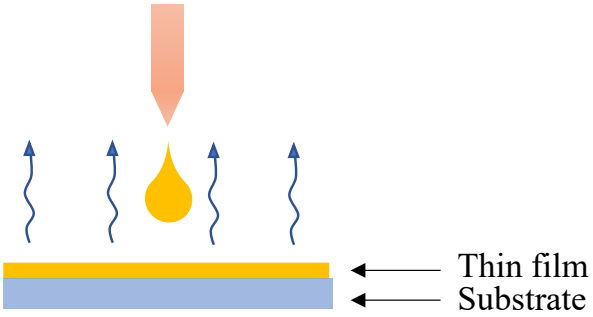

Fig. 14. Schematic diagram of the principle of drop casting technique.

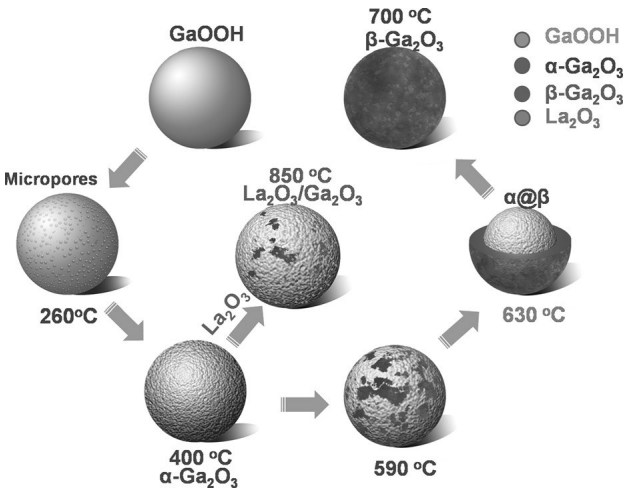

Fig. 15. Schematic diagram of the conversion of GaOOH to α-Ga_2O_3 and then to β-Ga_2O_3. Reprinted with permission from Ref. [91], © 2013 WILEY - VCH Verlag GmbH & Co. KGaA, Weinheim.

control the uniformity of the layer thickness. The thickness and properties of the film will be affected by the volume and concentration of the dispersion, the wetting of the substrate, the evaporation rate of the solvent and the overall drying process. In a number of studies, thin films of various materials have been obtained using this technique [85,86].

Pilliadugula et al. [87] investigated the sensing properties of β-Ga_2O_3 by drop-casting method. They prepared GaOOH powder from mixed solutions with different pH values by hydrothermal synthesis process, and then calcined it at 1000 °C for 5 hours to obtain white β-Ga_2O_3 powder. Then few drops of N-Methyl Pyrrolidone (NMP) were added to the β-Ga_2O_3 powder to obtain a paste of the desired consistency. The paste was drop-cast on the substrate, and finally the sensing semiconductor film was made by evaporating the solvent. Balasubramani et al. [88] also used a similar method to drop-cast a mixture of 5 wt.% β-Ga_2O_3/rGO (reduced graphene oxide) and 5 at.% α-terpineol on the alumina substrate to fabricate a gas sensor.

3.4. Different polymorphs of Ga_2O_3 obtained by sol-gel method

Many studies have shown that, in addition to β-Ga_2O_3, sol-gel method can be also used to prepare α-Ga_2O_3 [89–91] and γ-Ga_2O_3 [92–94] layers with reasonable quality. Areán et al. [92] prepared mesoporous γ-Ga_2O_3 by calcining gallium gel obtained by adding ammonia to ethanol solution of gallium nitrate. Delgado et al. [93] added ammonia water to the ethanol solution of gallium nitrate to prepare the γ-Ga_2O_3 polymorph and calcined it at 1073 K to obtain β-Ga_2O_3. Ristić et al. [89] added tetramethylammonium hydroxide ($N(CH_3)_4^+OH^-$, TMAH) solution to $GaCl_3$ solution to obtain α-GaOOH particles. These α-GaOOH particles transformed into single-phase α-Ga_2O_3 at 500 °C. When heated at 900 °C, the material of the particles exhibited phase transformation into β-Ga_2O_3. Wang et al. [91] dissolved gallium nitrate (20 g) in deionized water and stirred to form a solution. Further ammonia solution (5 wt.%) was added until the pH of the mixture reached 8.0. The resulting precipitate was filtered and dried to obtain GaOOH powder. As shown in Figure 15, they studied the conversion of GaOOH to α-Ga_2O_3 and β-Ga_2O_3.

Several studies [95–97] have shown that sol-gel synthesis conditions can influence structure of gallium oxide thin films and particles. Zhao et al. [95] used nonionic surfactant PEO (polyethylene oxide, Tergitol 15-S-7) and cationic surfactant CTAB (N-cetyl-N,N,N-trimethylammonium bromide, $C_{19}H_{42}NBr$) to prepare Ga_2O_3 particles with a porous structure. Surfactant-free synthesis can be used to obtain nonporous Ga_2O_3 particles. Chai et al. [96] prepared three polymorphs of gallium oxide (α, β, and α/β-Ga_2O_3) by adjusting the dosage of polyethylene glycol (PEG) 6000 by hydrothermal method. Sosnin et al. [97] proposed to explore chemical reaction between gallium nitrate and ammonia in aqueous solution to obtain oval acid-resistant microparticles of β-Ga_2O_3 after annealing the reaction deposit in air. The authors of this work found that the β-Ga_2O_3 particle size depends on the molar ratio of reacting substances in a non-monotonic manner, as shown in Figure 16.

4. APPLICATIONS IN BRIEF

Gallium oxide nanomaterials possess unique physical and chemical properties. They find practical applications in many fields, such as photocatalysis [98], ultraviolet detection [99], ultraviolet filters [100], flat panel displays [70], gas sensors [101] and optoelectronic devices [102]. They are also considered as some promising material candidates in the field of biomedicine. For example, Ga_2O_3 nanoparticles can carry drugs and penetrate cell membranes as a

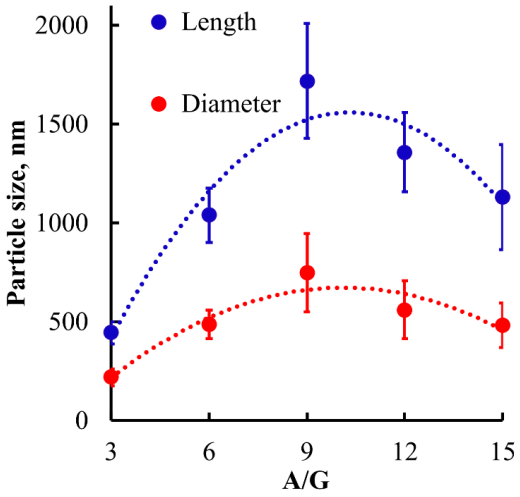

Fig. 16. Effect of the molar ratio of ammonia to gallium nitrate on the average size of β-Ga_2O_3 particles. Reprinted with permission from Ref. [97], © 2022 Elsevier B.V.

multifunctional drug carrier, and because of its excellent luminescent effect, the distribution of drugs in cells can be observed [103].

So far, there have been no extensive studies on the preparation of Ga_2O_3 thin films by the sol-gel method. At present status of sol-gel research, thin-film growth processes cannot be precisely controlled. However much lower costs of the sol-gel processing in comparison to vacuum-based synthesis methods dictate further development of research in the field. Ga_2O_3 films fabricated by the sol-gel method still contain defects, and the quality of the films needs to be improved. Ga_2O_3 based nanomaterials synthesized using solution-based methods have a high surface-to-volume ratio, which is important in photocatalysis [104–106] and sensor [71,107,108] applications. Being able to synthesize on a large scale is crucial for photoelectric conversion and photocatalysis [109]. Process simplification and minimization of defects in sol-gel fabricated Ga_2O_3 will facilitate its mass production.

5. CONCLUSION

In this brief review, we have highlighted the research status of gallium oxide prepared by sol-gel method. We have shown that Ga_2O_3 thin film structure is affected by the method of synthesis, the materials employed, the technique, and the process. Since gallium oxide materials can be used in applications such as deep ultraviolet detectors, PH sensors, gas sensors, photodegradation, and photocatalysis, the process of sol-gel method is worth investigating. We hope this review will serve as a reference for researchers using sol-gel methods.

ACKNOWLEDGMENTS

Authors acknowledge the support for this work from the Ministry of Science and Higher Education of the Russian Federation (agreement no. 075-15-2021-1349). X. Zhang was supported by the China Scholarship Council.

REFERENCES

[1] N. Stath, V. Härle, J. Wagner. *The status and future development of innovative optoelectronic devices based on III-nitrides on SiC and on III-antimonides*, Materials Science and Engineering: B, 2001, vol. 80, no. 1–3, pp. 224–231.

[2] K.A. Denault, M. Cantore, S. Nakamura, S.P. DenBaars, R. Seshadri. *Efficient and stable laser-driven white lighting*, AIP Advances, 2013, vol. 3, no. 7, art. no. 072107.

[3] J. Millán, P. Godignon, X. Perpiñà, A. Pérez-Tomás, J. Rebollo. *A survey of wide bandgap power semiconductor devices*, IEEE Transactions on Power Electronics, 2014, vol. 29, no. 5, pp. 2155–2163.

[4] Y. Li, X. Xiu, Z. Xiong, X. Hua, Z. Xie, P. Chen, B. Liu, T. Tao, R. Zhang, Y. Zheng, *Single-crystal GaN layer converted from β-Ga_2O_3 films and its application for free-standing GaN*, CrystEngComm, 2019, vol. 21, no. 8, pp. 1224–1230.

[5] S. Fujita, *Wide-bandgap semiconductor materials: For their full bloom*, Japanese Journal of Applied Physics, 2015, vol. 54, no. 3, art. no. 030101.

[6] B.J. Baliga, *Fundamentals of power semiconductor devices*, Springer New York, NY, 2008.

[7] H. Shiomi, Y. Nishibayashi, N. Fujimori, *Field-effect transistors using boron-doped diamond epitaxial films*, Japanese Journal of Applied Physics, 1989, vol. 28, no. 12A, pp. L2153–L2154.

[8] L. Boisbaudran, *On the chemical and spectroscopic characters of a new metal (gallium)*, The London, Edinburgh, and Dublin Philosophical Magazine and Journal of Science, 1875, vol. 50, no. 332, pp. 414–416.

[9] R. Roy, V.G. Hill, E.F. Osborn, *Polymorphism of Ga_2O_3 and the System Ga_2O_3–H_2O*, Journal of the American Chemical Society, 1952, vol. 74, no. 3, pp. 719–722.

[10] T. Oshima, T. Okuno, S. Fujita, *Ga_2O_3 thin film growth on c-plane sapphire substrates by molecular beam epitaxy for deep-ultraviolet photodetectors*, Japanese Journal of Applied Physics, 2007, vol. 46, no. 11R, pp. 7217–7220.

[11] T. Miyata, T. Nakatani, T. Minami, *Manganese-activated gallium oxide electroluminescent phosphor thin films prepared using various deposition methods*, Thin Solid Films, 2000, vol. 373, no. 1–2, pp. 145–149.

[12] J. Wang, L. Ye, X. Wang, H. Zhang, L. Li, C. Kong, W. Li, *High transmittance β-Ga_2O_3 thin films deposited by magnetron sputtering and post-annealing for solar-blind ultraviolet photodetector*, Journal of Alloys and Compounds, 2019, vol. 803, pp. 9–15.

[13] H.H. Tippins, *Optical absorption and photoconductivity in the band edge of β-Ga_2O_3*, *Physical Review*, 1965, vol. 140, no. 1A, pp. A316–A319.

[14] S.I. Stepanov, V.I. Nikolaev, V.E. Bougrov, A.E. Romanov, *Gallium Oxide: Properties and applications - a*

Review, Reviews on Advanced Materials Science, 2016, vol. 44, no. 1, pp. 63–86.

[15] P.N. Butenko, D.I. Panov, A.V. Kremleva, D.A. Zakgeim, A.V. Nashchekin, I.G. Smirnova, D.A. Bauman, A.E. Romanov, V.E. Bougrov, *Czochralski grown $(Al_xGa_{1-x})_2O_3$ crystals with variable Al content*, 2019, vol. 42, no. 6, pp. 802–807.

[16] S. Masuya, K. Sasaki, A. Kuramata, S. Yamakoshi, O. Ueda, M. Kasu, *Characterization of crystalline defects in β-Ga_2O_3 single crystals grown by edge-defined film-fed growth and halide vapor-phase epitaxy using synchrotron X-ray topography*, Japanese Journal of Applied Physics, 2019, vol. 58, no. 5, art. no. 055501.

[17] X. Du, Z. Li, C. Luan, W. Wang, M. Wang, X. Feng, H. Xiao, J. Ma, *Preparation and characterization of Sn-doped β-Ga_2O_3 homoepitaxial films by MOCVD*, Journal of Materials Science, 2015, vol. 50, no. 8, pp. 3252–3257.

[18] F.B. Zhang, K.Saito, T. Tanaka, M. Nishio, Q.X. Guo, *Structural and optical properties of Ga_2O_3 films on sapphire substrates by pulsed laser deposition*, Journal of Crystal Growth, 2014, vol. 387, pp. 96–100.

[19] A.S. Pratiyush, Z. Xia, S. Kumar, Y. Zhang, C. Joishi, R. Muralidharan, S. Rajan, D.N. Nath, *MBE-grown β-Ga_2O_3-based Schottky UV-C photodetectors with rectification ratio ~10^7*, IEEE Photonics Technology Letters, 2018, vol. 30, no. 23, pp. 2025–2028.

[20] K. Sasaki, M. Higashiwaki, A. Kuramata, T. Masui, S. Yamakoshi, *MBE grown Ga_2O_3 and its power device applications*, Journal of Crystal Growth, 2013, vol. 378, pp. 591–595.

[21] X. Zhang, D. Jiang, M. Zhao, H. Zhang, M. Li, M. Xing, Ji. Han, A. E. Romanov, *The effect of annealing temperature on Ga_2O_3 film properties*, Journal of Physics: Conference Series, 2021, vol. 1965, no. 1, art. no. 012066.

[22] S. Mobtakeri, Y. Akaltun, A. Özer, M. Kılıç, E.Ş. Tüzemen, E. Gür, *Gallium oxide films deposition by RF magnetron sputtering; a detailed analysis on the effects of deposition pressure and sputtering power and annealing*, Ceramics International, 2021, vol. 47, no. 2, pp. 1721–1727.

[23] H. Ma, H. Lu, T. Wang, J. Yang, X. Li, J. Chen, J. Tao, J. Zhu, Q. Guo, D.W. Zhang, *Precise control of the microstructural, optical, and electrical properties of ultrathin Ga_2O_3 film through nanomixing with few atom-thick SiO_2 interlayer via plasma enhanced atomic layer deposition*, Journal of Materials Chemistry C, 2018, vol. 6, no. 46, pp. 12518–12528.

[24] X. Li, H.-L. Lu, H.-P. Ma, J.-G. Yang, J.-X. Chen, W. Huang, Q. Guo, J.-J. Feng, D.W. Zhang, *Chemical, optical, and electrical characterization of Ga_2O_3 thin films grown by plasma-enhanced atomic layer deposition*, Current Applied Physics, 2019, vol. 19, no. 2, pp. 72–81.

[25] L.B. Cheah, R.A.M. Osman, P. Poopalan, *Ga_2O_3 thin films by sol-gel method its optical properties*, AIP Conference Proceedings, 2020, vol. 2203, no. 1, art. no. 020028.

[26] Y. Zhu, X. Xiu, F. Cheng, Y. Li, Z. Xie, T. Tao, P. Chen, B. Liu, R. Zhang, Y. Zheng, *Growth and nitridation of β-Ga_2O_3 thin films by sol-gel spin-coating epitaxy with post-annealing process*, Journal of Sol-Gel Science and Technology, 2021, vol. 100, no. 1, pp. 183–191.

[27] M. Bae, S. Kim, J. Baek, J. Koh, *Comparative study of high-temperature annealed and RTA process β-Ga_2O_3 thin film by sol–gel process*, Coatings, 2021, vol. 11, no. 10, art. no. 1220.

[28] Z. Galazka, *β-Ga_2O_3 for wide-bandgap electronics and optoelectronics*, Semiconductor Science and Technology, 2018, vol. 33, no. 11, art. no. 113001.

[29] F. Boschi, *Growth and investigation of different gallium oxide polymorphs*, Doctoral thesis, Universita' degli studi di Parma, 2017.

[30] H.Y. Playford, A.C. Hannon, E.R. Barney, R.I. Walton, *Structures of uncharacterised polymorphs of gallium oxide from total neutron diffraction*, Chemistry – A European Journal, 2013, vol. 19, no. 8, pp. 2803–2813.

[31] H.Y. Playford, A.C. Hannon, M.G. Tucker, D.M. Dawson, S.E. Ashbrook, R.J. Kastiban, J. Sloan, R.I. Walton, *Characterization of structural disorder in γ-Ga_2O_3*, The Journal of Physical Chemistry C, 2014, vol. 118, no. 29, pp. 16188–16198.

[32] I. Cora, F. Mezzadri, F. Boschi, M. Bosi, M. Čaplovičová, G. Calestani, I. Dódony, B. Pécz, R. Fornari, *The real structure of ε-Ga_2O_3 and its relation to κ-phase*, CrystEngComm, 2017, vol. 19, no. 11, pp. 1509–1516.

[33] M. Marezio, J.P. Remeika, Bond lengths in the α-Ga_2O_3 structure and the high-pressure phase of $Ga_{2-x}Fe_xO_3$, The Journal of Chemical Physics, 1967, vol. 46, no. 5, pp. 1862–1865.

[34] V.M. Bermudez, *The structure of low-index surfaces of β-Ga_2O_3*, Chemical Physics, 2006, vol. 323, no. 2–3, pp. 193–203.

[35] S. Yoshioka, H. Hayashi, A. Kuwabara, F. Oba, K. Matsunaga, I Tanaka, *Structures and energetics of Ga_2O_3 polymorphs*, Journal of Physics: Condensed Matter, 2007, vol. 19, no. 34, art. no. 346211.

[36] K. Akaiwa, S. Fujita, *Electrical conductive corundum-structured α-Ga_2O_3 thin films on sapphire with tin-doping grown by spray-assisted mist chemical vapor deposition*, Japanese Journal of Applied Physics, 2012, vol. 51, no. 7R, art. no. 070203.

[37] S. Lee, K. Akaiwa, S. Fujita, *Thermal stability of single crystalline alpha gallium oxide films on sapphire substrates*, Physica Status Solidi C, 2013, vol. 10, no. 11, pp. 1592–1595.

[38] S. Fujita, K. Kaneko, *Epitaxial growth of corundum-structured wide band gap III-oxide semiconductor thin films*, Journal of Crystal Growth, 2014, vol. 401, pp. 588–592.

[39] X. Chen, X. Yang, D. Zhou, S. Yang, F. Ren, H. Lu, K. Tang, S. Gu, R. Zhang, Y. Zheng, J. Ye, *Solar-blind photodetector with high avalanche gains and bias-tunable detecting functionality based on metastable phase α-Ga_2O_3/ZnO isotype heterostructures*, ACS Applied Materials & Interfaces, 2017, vol. 9, no. 42, pp. 36997–37005.

[40] V. Gottschalch, S. Merker, S. Blaurock, M. Kneiß, U. Teschner, M. Grundmann, H. Krautscheid, *Heteroepitaxial growth of α-, β-, γ- and κ-Ga_2O_3 phases by metalorganic vapor phase epitaxy*, Journal of Crystal Growth, 2019, vol. 510, pp. 76–84.

[41] H. Peelaers, C.G. Van de Walle, *Brillouin zone and band structure of β-Ga_2O_3*, Physica Status Solidi B, 2015, vol. 252, no. 4, pp. 828–832.

[42] Z. Galazka, K. Irmscher, R. Uecker, R. Bertram, M. Pietsch, A. Kwasniewski, M. Naumann, T. Schulz, R. Schewski, D. Klimm, M. Bickermann, *On the bulk β-Ga_2O_3*

single crystals grown by the Czochralski method, Journal of Crystal Growth, 2014, vol. 404, pp. 184–191.

[43] E.G. Víllora, K. Shimamura, T. Ujiie, K. Aoki, *Electrical conductivity and lattice expansion of β-Ga_2O_3 below room temperature*, Applied Physics Letters, 2008, vol. 92, no. 20, art. no. 202118.

[44] C. Janowitz, V. Scherer, M. Mohamed, A. Krapf, H. Dwelk, R. Manzke, Z. Galazka, R. Uecker, K. Irmscher, R. Fornari, M. Michling, D. Schmeißer, J.R. Weber, J.B. Varley, C.G. Van de Walle, *Experimental electronic structure of In_2O_3 and Ga_2O_3*, New Journal of Physics, 2011, vol. 13, no. 8, art. no. 085014.

[45] J.B. Varley, J.R. Weber, A. Janotti, C.G. Van de Walle, *Oxygen vacancies and donor impurities in β-Ga_2O_3*, Applied Physics Letters, 2010, vol. 97, no. 14, art. no. 142106.

[46] Z. Galazka, *Growth of bulk β-Ga_2O_3 single crystals by the Czochralski method*, Journal of Applied Physics, 2022, vol. 131, no. 3, art. no. 031103.

[47] Z. Galazka, R. Uecker, K. Irmscher, M. Albrecht, D. Klimm, M. Pietsch, M. Brützam, R. Bertram, S. Ganschow, R. Fornari, *Czochralski growth and characterization of β-Ga_2O_3 single crystals*, Crystal Research and Technology, 2010, vol. 45, no. 12, pp. 1229–1236.

[48] J. Zhang, B. Li, C. Xia, G. Pei, Q. Deng, Z. Yang, W. Xu, H. Shi, F. Wu, Y. Wu, J. Xu, *Growth and spectral characterization of β-Ga_2O_3 single crystals*, Journal of Physics and Chemistry of Solids, 2006, vol. 67, no. 12, pp. 2448–2451.

[49] N. Ueda, H. Hosono, R. Waseda, H. Kawazoe, *Anisotropy of electrical and optical properties in β-Ga_2O_3 single crystals*, Applied Physics Letters, 1997, vol. 71, no. 7, pp. 933–935.

[50] E.G. Víllora, M. Yamaga, T. Inoue, S. Yabasi, Y. Masui, T. Sugawara, T. Fukuda, *Optical spectroscopy study on β-Ga_2O_3*, Japanese Journal of Applied Physics, 2002, vol. 41, no. 6A, L622–L625.

[51] T. Harwig, F. Kellendonk, S. Slappendel. *The ultraviolet luminescence of β-galliumsesquioxide*, Journal of Physics and Chemistry of Solids, 1978, vol. 39, no. 6, pp. 675–680.

[52] J.B. Varley, A. Janotti, C. Franchini, C.G. Van De Walle, *Role of self-trapping in luminescence and p-type conductivity of wide-band-gap oxides*, Physical Review B, 2012, vol. 85, no. 8, art. no. 081109.

[53] V. Vasyltsiv, L. Kostyk, O. Tsvetkova, R. Lys, M. Kushlyk, B. Pavlyk, A. Luchechko, *Luminescence and conductivity of β-Ga_2O_3 and β-Ga_2O_3:Mg single crystals*, Acta Physica Polonica A, 2022, vol. 141, no. 4, pp. 312–318.

[54] T. Onuma, S. Fujioka, T. Yamaguchi, M. Higashiwaki, K. Sasaki, T. Masui, T. Honda, *Correlation between blue luminescence intensity and resistivity in β-Ga_2O_3 single crystal*, Applied Physics Letters, 2013, vol. 103, no. 4, art. no. 041910.

[55] S.J. Pearton, J. Yang, P.H. Cary, F. Ren, J. Kim, M.J. Tadjer, M.A. Mastro, *A review of Ga_2O_3 materials, processing, and devices*, Applied Physics Reviews, 2018, vol. 5, no. 1, art. no. 011301.

[56] M. Higashiwaki, K. Sasaki, H. Murakami, Y. Kumagai, A. Koukitu, A. Kuramata, T. Masui, S. Yamakoshi, *Recent progress in Ga_2O_3 power devices*, Semiconductor Science and Technology, 2016, vol. 31, no. 3, art. no. 034001.

[57] M. Higashiwaki, K. Sasaki, A. Kuramata, T. Masui, S. Yamakoshi, *Gallium oxide (Ga_2O_3) metal-semiconductor field-effect transistors on single-crystal β-Ga_2O_3 (010) substrates*, Applied Physics Letters, 2012, vol. 100, no. 1, art. no. 013504.

[58] K. Sasaki, A. Kuramata, T. Masui, E.G. Víllora, K. Shimamura, S. Yamakoshi, *Device-quality β-Ga_2O_3 epitaxial films fabricated by ozone molecular beam epitaxy*, Applied Physics Express, 2012, vol. 5, no. 3, art. no. 035502.

[59] Z. Guo, A. Verma, X. Wu, F. Sun, A. Hickman, T. Masui, A. Kuramata, M. Higashiwaki, D. Jena, T. Luo, *Anisotropic thermal conductivity in single crystal β-gallium oxide*, Applied Physics Letters, 2015, vol. 106, no. 11, art. no. 111909.

[60] K. Adachi, H. Ogi, N. Takeuchi, N. Nakamura, H. Watanabe, T. Ito, Y. Ozaki, *Unusual elasticity of monoclinic β−Ga_2O_3*, Journal of Applied Physics, 2018, vol. 124, no. 8, art. no. 085102.

[61] S. Luan, L. Dong, R. Jia, *Analysis of the structural, anisotropic elastic and electronic properties of β-Ga_2O_3 with various pressures*, Journal of Crystal Growth, 2019, vol. 505, pp. 74–81.

[62] S.S. Kistler, *Coherent expanded aerogels and jellies*, Nature, 1931, vol. 127, no. 3211, pp. 741.

[63] S. Sakka, *History of the sol-gel chemistry and technology*, in: *Handbook of sol-gel science and technology*, ed. by L. Klein, M. Aparicio, A. Jitianu, Springer, Cham, 2018, pp. 3–29.

[64] Y. Dimitriev, Y. Ivanova, R. Iordanova, *History of sol-gel science and technology*, Journal of the University of Chemical Technology and Metallurgy, 2008, vol. 43, no. 2, pp. 181–192.

[65] M. Yada, H. Takenaka, M. Machida, T. Kijima, *Mesostructured gallium oxides templated by dodecyl sulfate assemblies*, Journal of the Chemical Society, Dalton Transactions, 1998, no. 10, pp. 1547–1550.

[66] L.L. Hench, J.K. West, *The sol-gel process*, Chemical Reviews, 1990, vol. 90, no. 1, pp. 33–72.

[67] Q. Liu, *Preparation of NiO thin film by sol-gel spin coating method and its light transmission properties*, Diss. Liaoning Normal University.

[68] Y. Liu, *GaO reaction self-assembly to form GaN particles prepared by sol-gel method*, Diss. Shandong Normal University.

[69] A. Mohammadzadeh, S.K. Naghib Zadeh, M.H. Saidi, M. Sharifzadeh, *Chapter 3 – Mechanical engineering of solid oxide fuel cell systems: geometric design, mechanical configuration, and thermal analysis*, in: *Design and Operation of Solid Oxide Fuel Cells*, Woodhead Publishing Series in Energy, Academic Press, 2020, pp. 85–130.

[70] T. Minami, T. Shirai, T. Nakatani, T. Miyata, *Electroluminescent devices with Ga_2O_3:Mn thin-film emitting layer prepared by sol-gel process*, Japanese Journal of Applied Physics, 2000, vol. 39, no. 6A, L524–L526.

[71] M.R. Mohammadi, D.J. Fray, *Semiconductor TiO_2–Ga_2O_3 thin film gas sensors derived from particulate sol–gel route*, Acta Materialia, 2007, vol. 55, no. 13, pp. 4455–4466.

[72] G. Sinha, A. Datta, S.K. Panda, P.G. Chavan, M.A More, D.S. Joag, A. Patra, *Self-catalytic growth and field-emission properties of Ga_2O_3 nanowires*, Journal of Physics D: Applied Physics, 2009, vol. 42, no. 18, art. no. 185409.

[73] X. Li, D. Bi, C. Yi, J. Decoppet, J. Luo, S. Zakeeruddin, A. Hagfeldt, M. Gratzel, *A vacuum flash-assisted solution process for high-efficiency large-area perovskite solar cells*, Science, 2016, vol. 353, no. 6294, pp. 58–62.

[74] Y. Kokubun, K. Miura, F. Endo, S. Nakagomi, *Sol-gel prepared β-Ga_2O_3 thin films for ultraviolet photodetectors*, Applied Physics Letters, 2007, vol. 90, no. 3, art. no. 031912.

[75] M. Fleischer, W. Hanrieder, H. Meixner, *Stability of semiconducting gallium oxide thin films*, Thin Solid Films, 1990, vol. 190, no. 1, pp. 93–102.

[76] G.A. Battiston, R. Gerbasi, M. Porchia, R. Bertoncello, F. Caccavale, *Chemical vapour deposition and characterization of gallium oxide thin films*, Thin Solid Films, 1996, vol. 279, no. 1–2, pp. 115–118.

[77] H. Shen, Y. Yin, K. Tian, K. Baskaran, L. Duan, X. Zhao, A. Tiwari, *Growth and characterization of β-Ga_2O_3 thin films by sol-gel method for fast-response solar-blind ultraviolet photodetectors*, Journal of Alloys and Compounds, 2018, vol. 766, pp. 601–608.

[78] Y. Li, A. Trinchi, W. Wlodarski, K. Galatsis, K. Kalantar-zadeh, *Investigation of the oxygen gas sensing performance of Ga_2O_3 thin films with different dopants*, Sensors and Actuators B: Chemical, 2003, vol. 93, no. 1–3, pp. 431–434.

[79] J.P. Sawant, H.M. Pathan, R.B. Kale, *Spray pyrolytic deposition of $CuInS_2$ thin films: properties and applications*, Engineered Science, 2021, vol. 13, pp. 51–64.

[80] P.S. Patil, *Versatility of chemical spray pyrolysis technique*, Materials Chemistry and Physics, 1999, vol. 59, no. 3, pp. 185–198.

[81] S.P.S Arya, H.E Hintermann, *Growth of Y-Ba-Cu-O superconducting thin films by ultrasonic spray pyrolysis*, Thin Solid Films, 1990, vol. 193–194, pp. 841–846.

[82] C. Chen, *Electrostatic spray deposition of thin layers of cathode materials for lithium battery*, Solid State Ionics, 1996, vol. 86–88, pp. 1301–1306.

[83] G. Gan, Y. Guo, *Sol-gel film preparation process and its application*, Journal of Kunming University of Science and Technology, 1997, vol. 22, no. 1, pp. 142–145.

[84] D.I. Panov, X. Zhang, V.A. Spiridonov, L.V. Azina, R.K. Nuryev, N.D. Prasolov, L.A. Sokura, D.A. Bauman, V.E. Bougrov, A.E. Romanov, *Thin films of gallium oxide obtained by spray-pyrolysis: method and properties*, Materials Physics and Mechanics, 2022, vol. 50, no. 1, pp. 107–117.

[85] J. Park, S. Lee, H.H. Lee, *High-mobility polymer thin-film transistors fabricated by solvent-assisted drop-casting*, Organic Electronics, 2006, vol. 7, no. 5, pp. 256–260.

[86] A.A.M. Farag, I.S. Yahia, *Structural, absorption and optical dispersion characteristics of rhodamine b thin films prepared by drop casting technique*, Optics Communications, 2010, vol. 283, no. 21, pp. 4310–4317.

[87] R. Pilliadugula, N.G. Krishnan, *Effect of pH dependent morphology on room temperature NH_3 sensing performances of β-Ga_2O_3*, Materials Science in Semiconductor Processing, 2020, vol. 112, art. no. 105007.

[88] V. Balasubramani, A. Nowshath Ahamed, S. Chandraleka, K. Krishna Kumar, M.R. Kuppusamy, T.M. Sridhar, *Highly sensitive and selective H_2S gas sensor fabricated with β-Ga_2O_3 /rGO*, ECS Journal of Solid State Science and Technology, 2020, vol. 9, no. 5, art. no. 055009.

[89] M. Ristić, S. Popović, S. Musić, *Application of sol–gel method in the synthesis of gallium(III)-oxide*, Materials Letters, 2005, vol. 59, no. 10, pp. 1227–1233.

[90] Y. Hou, L. Wu, X. Wang, Z. Ding, Z. Li, X. Fu, *Photocatalytic performance of α-, β-, and γ-Ga_2O_3 for the destruction of volatile aromatic pollutants in air*, Journal of Catalysis, 2007, vol. 250, no. 1, pp. 12–18.

[91] X. Wang, Q. Xu, F. Fan, X. Wang, M. Li, Z. Feng, C. Li, *Study of the phase transformation of single particles of Ga_2O_3 by UV-Raman spectroscopy and high-resolution TEM*, Chemistry – An Asian Journal, 2013, vol. 8, no. 9, pp. 2189–2195.

[92] C.O. Areán, A.L. Bellan, M.P. Mentruit, M.R. Delgado, G.T. Palomino, *Preparation and characterization of mesoporous γ-Ga_2O_3*, Microporous and Mesoporous Materials, 2000, vol. 40, no. 1–3, pp. 35–42.

[93] M.R. Delgado, C.O. Areán, *Surface chemistry and pore structure of β-Ga_2O_3*, Materials Letters, 2003, vol. 57, no. 15, pp. 2292–2297.

[94] M. Hirano, K. Sakoda, Y. Hirose, *Direct formation and phase stability of luminescent γ-Ga_2O_3 spinel nanocrystals via hydrothermal method*, Journal of Sol-Gel Science and Technology, 2016, vol. 77, no. 2, pp. 348–354.

[95] Y. Zhao, R.L. Frost, W.N. Martens, *Synthesis and characterization of gallium oxide nanostructures via a soft-chemistry route*, The Journal of Physical Chemistry C, 2007, vol. 111, no. 44, pp. 16290–16299.

[96] X. Chai, Z. Liu, Y. Huang, *Influence of PEG 6000 on gallium oxide (Ga_2O_3) polymorphs and photocatalytic properties*, Science China Chemistry, 2015, vol. 58, no. 3, pp. 532–538.

[97] I.M. Sosnin, L.A. Sokura, M.V. Dorogov, I.G. Smirnova, A.E. Romanov, *Aqueous solution synthesis and size control of acid-resistant β-Ga_2O_3 microparticles*, Materials Letters, 2023, vol. 335, art. no. 133758.

[98] M. Jędrzejczyk, K. Zbudniewek, J. Rynkowski, V. Keller, J. Grams, A.M. Ruppert, N. Keller, *Wide band gap Ga_2O_3 as efficient UV-C photocatalyst for gas-phase degradation applications*, Environmental Science and Pollution Research, 2017, vol. 24, no. 34, pp. 26792–26805.

[99] D. Zhang, W. Zheng, R.C. Lin, T.T. Li, Z.J. Zhang, F. Huang, *High quality β-Ga_2O_3 film grown with N_2O for high sensitivity solar-blind-ultraviolet photodetector with fast response speed*, Journal of Alloys and Compounds, 2018, vol. 735, pp. 150–154.

[100] Z. Ji, J. Du, J. Fan, W. Wang, *Gallium oxide films for filter and solar-blind UV detector*, Optical Materials, 2006, vol. 28, no. 4, pp. 415–417.

[101] M. Fleischer, H. Meixner, *Gallium oxide thin films: A new material for high-temperature oxygen sensors*, Sensors and Actuators B: Chemical, 1991, vol. 4, no. 3–4, pp. 437–441.

[102] B. Zhao, F. Wang, H. Chen, L. Zheng, L. Su, D. Zhao, X. Fang, *An ultrahigh responsivity (9.7 mA W^{-1}) self-powered solar-blind photodetector based on individual ZnO–Ga_2O_3 heterostructures*, Advanced Functional Materials, 2017, vol. 27, no. 17, art. no. 1700264.

[103] X. Wang, J. Situ, X. Ying, H. Chen, H. Pan, Y. Jin, Y. Du, *β-Ga_2O_3:Cr^{3+} nanoparticle: A new platform with near infrared photoluminescence for drug targeting delivery and bio-imaging simultaneously*, Acta Biomaterialia, 2015, vol. 22, pp. 164–172.

[104] W. Zhao, Y. Yang, R. Hao, F. Liu, Y. Wang, M. Tan, J. Tang, D. Ren, D. Zhao, *Synthesis of mesoporous β-Ga_2O_3*

nanorods using PEG as template: preparation, characterization and photocatalytic properties, Journal of Hazardous Materials, 2011, vol. 192, no. 3, pp. 1548–1554.

[105] S. Kim, H. Ryou, I.G. Lee, M. Shin, B.J. Cho, W.S. Hwang, *Impact of Al doping on a hydrothermally synthesized β-Ga_2O_3 nanostructure for photocatalysis applications*, RSC Advances, 2021, vol. 11, no. 13, pp. 7338–7346.

[106] K. Girija, S. Thirumalairajan, A.K. Patra, D. Mangalaraj, N. Ponpandian, C. Viswanathan, *Enhanced photocatalytic performance of novel self-assembled floral β-Ga_2O_3 nanorods*, Current Applied Physics, 2013, vol. 13, no. 4, pp. 652–658.

[107] R. Pilliadugula, N.G. Krishnan, *Gas sensing performance of GaOOH and β-Ga_2O_3 synthesized by hydrothermal method: a comparison*, Materials Research Express, 2018, vol. 6, no. 2, art. no. 025027.

[108] B. Zhang, H. Lin, H. Gao, X. Lu, C. Nam, P. Gao, *Perovskite-sensitized β-Ga_2O_3 nanorod arrays for highly selective and sensitive NO_2 detection at high temperature*, Journal of Materials Chemistry A, 2020, vol. 8, no. 21, pp. 10845–10854.

[109] M. Fleischer, H. Meixner, *Oxygen sensing with long-term stable Ga_2O_3 thin films*, Sensors and Actuators B: Chemical, 1991, vol. 5, no. 1–4, pp. 115–119.

УДК 548.524

Приготовление тонких пленок Ga_2O_3 золь-гель методом — краткий обзор

X. Zhang[1], В.А. Спиридонов[1], Д.Ю. Панов[1], И.М. Соснин[1,2], А.Е. Романов[1,2,3]

[1] Университет ИТМО, Кронверкский пр., д. 49, лит. А, Санкт-Петербург, 197101, Россия
[2] Тольяттинский государственный университет, Белорусская ул., д. 14, Тольятти, 445020, Россия
[3] ФТИ им. А.Ф. Иоффе, Политехническая ул., д. 26, Санкт Петербург 194021, Россия

Аннотация. В настоящее время оксид галлия (Ga_2O_3) как широкозонный полупроводниковый материал привлекает все большее внимание в различных практических областях. В связи с этим было предпринято много усилий по изготовлению и исследованию его объемного кристалла, тонких пленок и нанопроволок. Для пленок Ga_2O_3 существует множество методов подготовки, таких как осаждение металлорганических соединений из газообразной фазы, хлорид-гидридная газофазная эпитаксия, импульсное лазерное напыление, молекулярно-пучковая эпитаксия, радиочастотное магнетронное напыление, атомно-слоевое осаждение, мокрая химия и золь-гель. Этот краткий обзор посвящен приготовлению тонких пленок Ga_2O_3 золь-гель методами. Золь-гель методы включают нанесение покрытия погружением, центрифугирование, спрей-пиролиз и метод капельного литья. В работе обобщены и проанализированы детали изготовления тонких пленок β-Ga_2O_3 золь-гель методом. Обсуждаются полиморфизм, структура и свойства полученных методом золь-гель пленок Ga_2O_3.

Ключевые слова: золь-гель; Ga_2O_3; тонкая пленка